PAPER

A PCB-Integratable Metal Cap Slot Antenna for 60-GHz Band Mobile Terminals

Takashi TOMURA[†a)], **Haruhisa HIRAYAMA**[†], ***Members***, ***and*** **Jiro HIROKAWA**[†], ***Fellow***

SUMMARY A PCB-integratable metal cap slot antenna is developed for the 60-GHz band. The antenna is composed of two slots and a T-junction and is fed by a post-wall waveguide on a substrate. The dimensions of the designed antenna are $8.0 \times 4.5 \times 2.5\,\mathrm{mm}^3$. The designed antenna is insensitive with a metal block behind the antenna. The designed antenna is fabricated by machining a brass block and evaluated by measurement. The measurement shows reflection less than −10.0 dB, gain larger than 7.8 dBi and beamwidth between 54°–65° over the 60-GHz band with endfire radiation. The antenna showed high gain together with short length of half wavelength in the radiation direction. This antenna also can be integrated with printed circuit board (PCB) and is suitable for mobile terminals such as smart phones and tablets.

key words: *endfire antenna, metal cap antenna, millimeter wave, slot antenna*

1. Introduction

Demands for high-speed wireless communication have increased because of widespread mobile terminals such as smart phones and tablets. The 60-GHz band, 57–66 GHz, is allocated worldwide for wireless communication and can be used without license [1]. One of the application is data transfer from a fixed terminal to mobile terminals or between mobile terminals. The feature of the application is that communication partner can be selected spatially by pointing the mobile terminal toward the communication partner. For such application, antennas whose radiation direction is single and parallel to PCB (hereinafter called endfire radiation) are suitable rather than boresight radiation antennas. Furthermore, the beamwidth of two orthogonal planes should be same because we do not know how users hold a wireless terminal.

Two types of millimeter wave endfire antennas constructed on a substrate have been studied: patch array type and aperture type. The patch array includes Yagi-Uda antennas [2]–[4], dipole antennas [5]–[7], a patch antenna [8] and bow-tie antennas [9]. The aperture type antenna includes tapered slot antennas [10], horn antennas [11] and substrate slab antennas [12]. These antennas realize endfire radiation by increasing the number of array elements or their dimension on a substrate. A serious drawback of these antennas is that radiation pattern is disturbed when an object or an electrical circuit part is placed over the antennas. In [4], shielded Yagi-Uda antennas were proposed that are insensitive to their surroundings. However, the antenna has to be isolated from PCB and so cannot be integrated with PCB. Furthermore, its dimension in the radiation direction is long because endfire radiation is realized by placing array elements in the radiation direction.

We have proposed a metal cap antenna [13] to address these problems. The metal cap antenna is composed of two slots and a waveguide T-junction and fed by a micro strip line (MSL) on a substrate. The metal cap antenna has short length in radiation direction. A metal block behind the antenna does not affect the radiation pattern of the antenna because the electromagnetic field is confined in the waveguide. However, the edge of the substrate has to be machined to insert itself to the metal cap antenna. Measurement results showed degradation in the realized gain and reflection because accurate machining is required.

The main contribution of this paper is to present a simple antenna structure with robustness on fabrication tolerance and effects from surrounding objects in the 60-GHz band. We present a post-wall waveguide (PWW) feed PCB-integratable metal cap antenna [14], which does not require machining a substrate and is robust on fabrication tolerance. The proposed antenna is designed and evaluated by measurement. Different from [14], measurement results of the fabricated antenna are shown and effectiveness of the proposed antenna is presented.

2. Antenna Structure

The structure of the proposed antenna is shown in Fig. 1. The antenna is composed of a substrate and a metal cap antenna. The substrate is ceramic-filled PTFE and its thickness is 0.21 mm with 18-μm copper clad. The dielectric constant and loss tangent of the substrate is 4.1 and 0.0081, which is estimated by measurement written in Sect. 4. The substrate consists of a MSL, a PWW and a MSL-PWW transition to feed the metal cap antenna. A matching post is located in the PWW for reflection canceling. The metal cap antenna is composed of a T-junction and two slots. Power fed by the substrate is divided into two by the T-junction and the two slots are excited with uniform amplitude and phase. Two slots are employed to increase directivity and realize same beamwidth in both E- and H-planes. The substrate is inserted into the metal cap until it touches the metal cap antenna. This structure realizes robustness against fabrication

Manuscript received March 12, 2018.
Manuscript revised June 26, 2018.
Manuscript publicized August 13, 2018.

[†]The authors are with the Department of Electrical and Electronic Engineering, Tokyo Institute of Technology, Tokyo, 152-8552 Japan.
a) E-mail: tomura@ee.e.titech.ac.jp

DOI: 10.1587/transcom.2018EBP3070

Copyright © 2019 The Institute of Electronics, Information and Communication Engineers

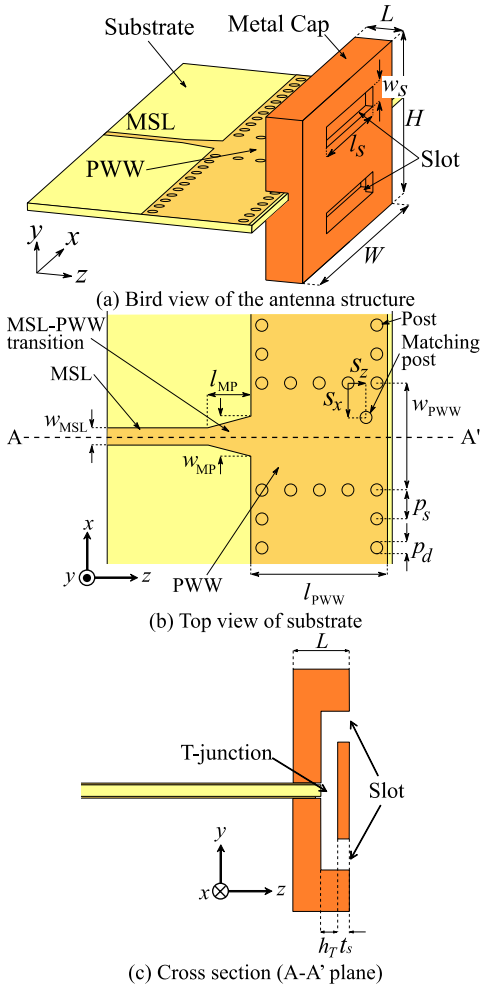

Fig. 1 Post-wall waveguide slot array antenna.

Table 1 Parameters.

Component	Quantity	Symbol	Value (mm)
Slot	Length	l_s	4.53
	Width	w_s	0.57
	Thickness	t_s	0.20
Metal block	Width	W	8.01
	Height	H	4.45
	Length	L	2.52
T-junction	Height of waveguide	h_T	0.32
Matching post	x-position	s_x	0.72
	z-position	s_z	0.38
PWW	Width	w_{PWW}	2.32
	Length	l_{PWW}	4.05
	Post diameter	p_d	0.25
	Post spacing	p_s	0.60
MSL	Strip width	w_{MSL}	0.356
MSL-PWW transition	Length	l_{MP}	0.92
	Strip width at PWW side	w_{MP}	0.80

tolerance.

3. Design

The metal cap antenna and the feed structure are designed so

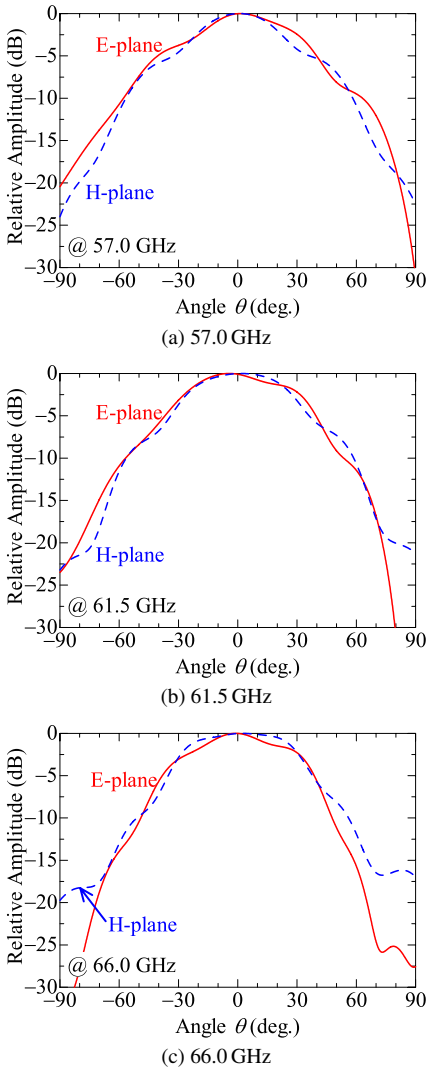

Fig. 2 Simulated radiation pattern.

Table 2 Designed half power beamwidth.

Cut-plane	57 GHz	61.5 GHz	66 GHz
E	55.6°	62.9°	62.8°
H	47.3°	56.9°	62.7°

that low reflection (< -10 dB), endfire radiation and same beamwidth between E- and H-plane are realized over the target bandwidth, 57–66 GHz. HFSS, a simulator based on finite element method, is used for analysis.

3.1 Antenna

The antenna is designed as follows. At first, the dimensions of the slots and the external form of the metal cap antenna are determined to satisfy desired radiation characteristics. Next, the dimensions of the T-junction and the matching post are adjusted for broadband low reflection characteristics.

To realize endfire radiation and same beamwidth over the bandwidth, four parameters are adjusted: the metal

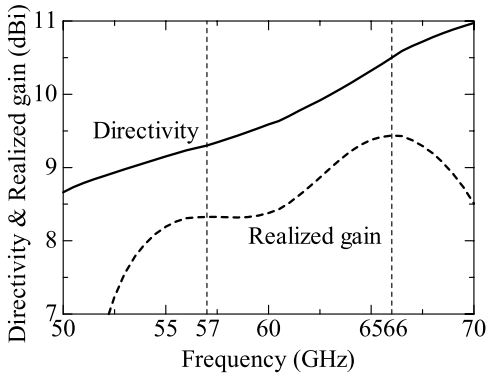

Fig. 3 Frequency characteristic of directivity and realized gain.

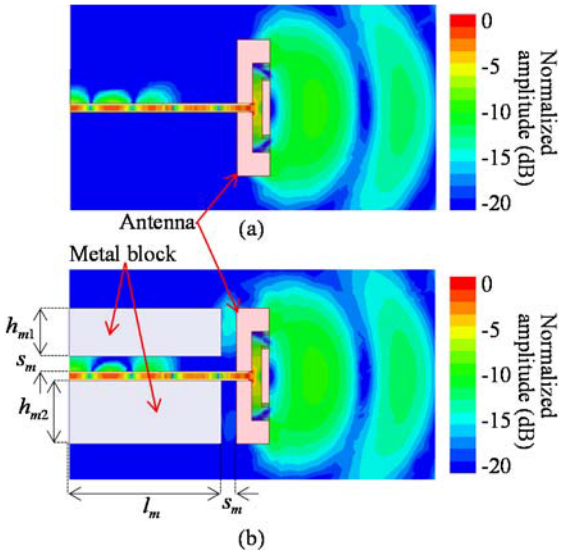

Fig. 4 Electromagnetic field distribution (a) without a metal block, (b) with metal blocks (h_{m1} = 1.58 mm, h_{m2} = 2.08 mm, l_m = 4.95 mm, s_m = 0.5 mm).

block dimensions H, L, W and slot length l_s while element spacing and slot width are kept 2.35 mm (0.48 λ_0 at the center frequency) and 0.57 mm, respectively. Designed parameters are shown in Table 1. The slot length is 0.93 λ_0 at the center frequency. Radiation patterns and beamwidth over the bandwidth are shown in Fig. 2 and Table 2, respectively. The radiation patterns on both E- and H-plane have a single peak and same beamwidth. Frequency characteristics of directivity are shown in Fig. 3. The directivity is more than 9.3 dBi over the target bandwidth.

The antenna with metal blocks behind the antenna is simulated to evaluate the effect of a metal block such as electrical parts or integral circuits. Electromagnetic field distribution of both cases are shown in Fig. 4. Electromagnetic field behind the antenna and above and below the MSL is less than −20 dB. That is why the effect of the metal blocks on the field is small. Employment of the PWW and the waveguide slot structure realizes such low electromagnetic field because all of the electromagnetic field is confined in the PWW or the waveguide. The radiation pattern at the

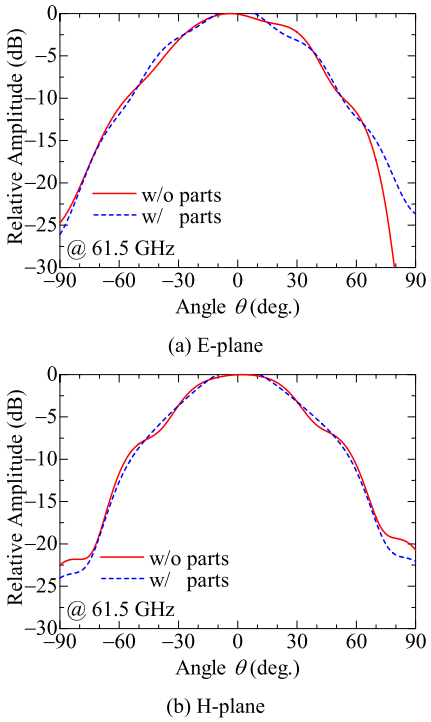

Fig. 5 Effect of metal block on radiation pattern.

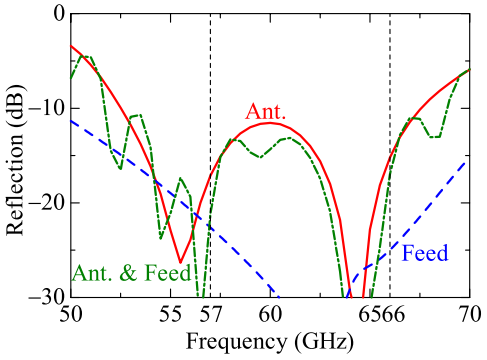

Fig. 6 Frequency characteristic of reflection.

center frequency are shown in Fig. 5. The effect of the metal blocks on the radiation pattern is negligible. Therefore, the antenna is insensitive with a metal block behind the antenna.

To realize broadband characteristics of reflection, four parameters are adjusted: the WG height of the T-junction h_T, the thickness of the slot plate t_s, position of the matching post s_x and s_z. h_T is designed as large as possible to decrease the effect of the fabrication tolerance. The matching post works as an inductive element and its inductance increases as s_x increases [15]. s_z changes the distance between the matching post and the T-junction. The designed parameters are listed in Table 1. Frequency characteristics of reflection and realized gain are shown in Fig. 6 and Fig. 3, respectively. The reflection is less than −11.5 dB and the realized gain more than 8.3 dBi over the target bandwidth. Effect of fabrication tolerance on the reflection is shown in Fig. 7. The reflection is kept less than −10 dB in the tar-

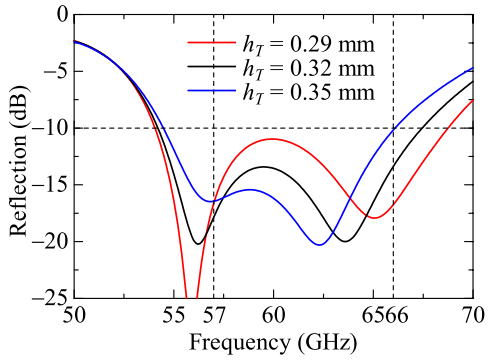

(a) Waveguide height h_T

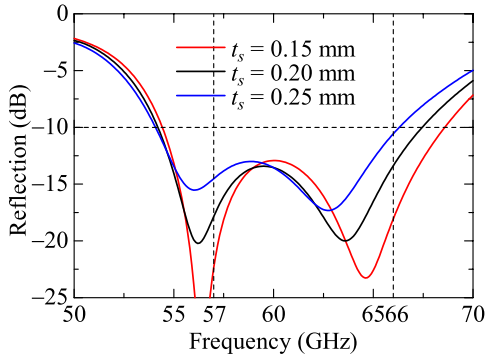

(b) Slot plate thickness t_s

Fig. 7 Effect of fabrication tolerance on reflection.

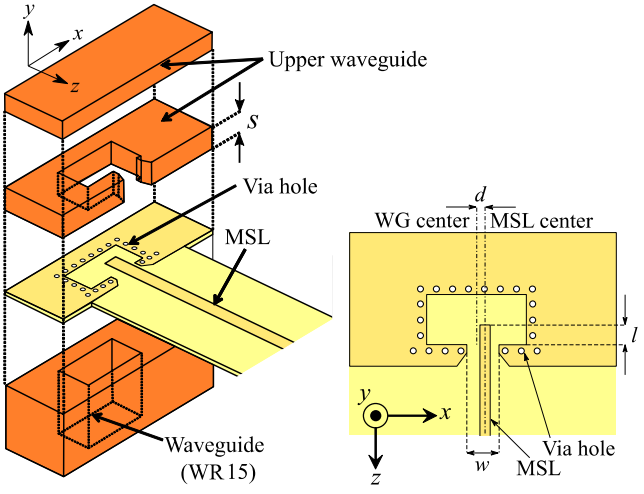

Fig. 8 Waveguide-microstrip line transition.

Table 3 Designed parameters of the feed circuit.

Symbol	Quantity	Value (mm)
d	Displacement of MSL center	0.25
l	Length of MSL in WG region	0.75
s	Back short length of the WG	0.55
w	Width of waveguide aperture	1.20

get bandwidth against ±0.03-mm errors of the height of the T-junction h_T and ±0.05-mm errors of thickness of the slot plate t_s. The WG height of the T-junction h_T is increased from 0.20 mm [13] to 0.32 mm. This increment improves

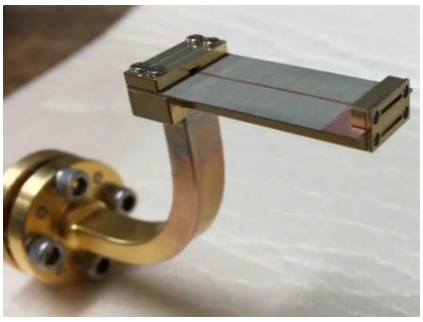

Fig. 9 Fabricated antenna.

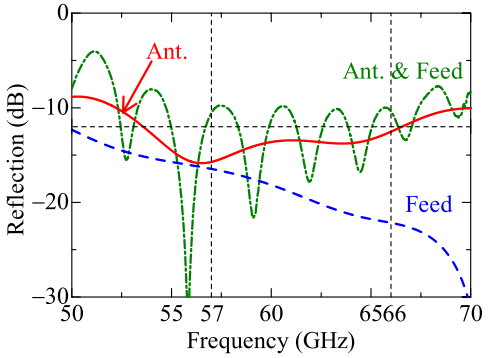

Fig. 10 Measured frequency characteristic of reflection.

robustness on fabrication tolerance.

3.2 Feed Circuit

Waveguide to microstrip line (WG-MSL) transition [16] is designed for feed the metal cap antenna. The structure of the transition is shown in Fig. 8. The parameters are designed so that the transmission is maximized. The designed parameters and frequency characteristics of reflection are shown in Table 3 and Fig. 6, respectively. Reflection is less than −20.7 dB over the target bandwidth. Total reflection of the antenna and feed circuit is shown in the same figure. Reflection is suppressed less than −13.1 dB over the target bandwidth.

4. Experimental Results

The designed antenna with the feed circuit is fabricated as shown in Fig. 9. The metal cap antenna and a part of the WG-MSL transition is fabricated by machining brass. The metal cap antenna is composed of three parts, which are fixed by screws. The dimension of the metal cap antenna is $8.0 \times 4.5 \times 2.5\,\text{mm}^3$.

Measured frequency characteristics of reflection are shown in Fig. 10. The reflection of the antenna and feed parts was extracted by gating time domain response. The time ranges for the time-gaiting windows for the feed and the antenna parts are 0 ns to 0.23 ns and 0.23 ns to 0.40 ns, respectively. The reflection of the antenna is less than

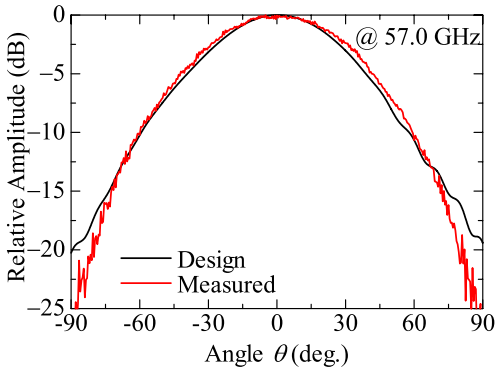

(a-1) 57.0 GHz, E-plane

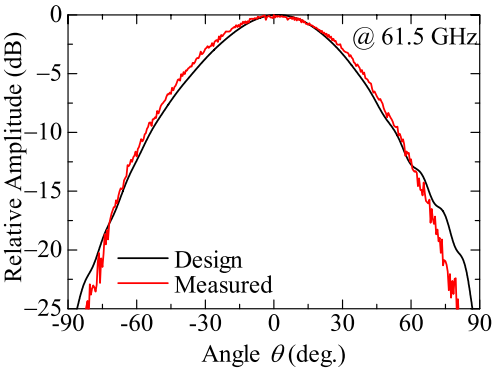

(b-2) 61.5GHz, H-plane

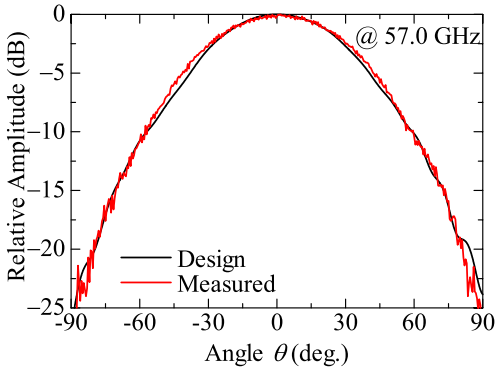

(a-2) 57.0 GHz, H-plane

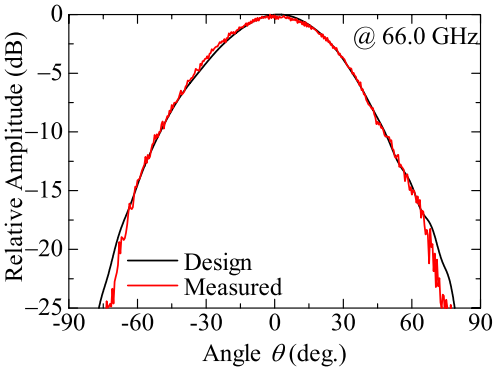

(c-1) 66.0GHz, H-plane

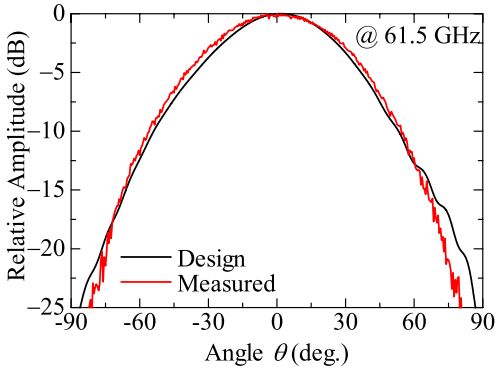

(b-1) 61.5GHz, E-plane

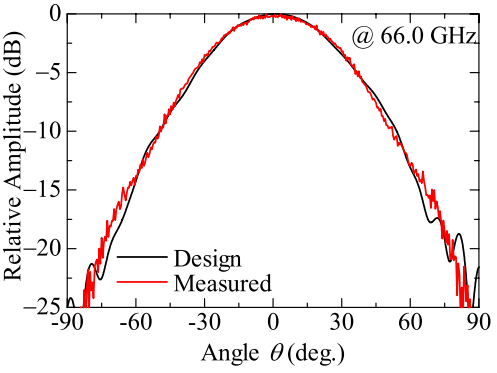

(c-2) 66.0GHz, H-plane

Fig. 11 Measured radiation pattern.

Table 4 Measured half power beamwidth.

Cut-plane	57 GHz	61.5 GHz	66 GHz
E	64.7°	60.6°	54.1°
H	65.3°	63.0°	56.6°

−10.0 dB from 52.2 to 70 GHz. The robustness on the fabrication tolerance is confirmed unlike the measured reflection of the previous antenna [13] which was degraded up to −6.0 dB. 3.3-GHz span ripple is observed in antenna and feed reflection. The span indicates multiple reflection from two points separated by 22.5 mm. The distance between the WG-MSL transition and the antenna is 22.2 mm. Therefore, the ripple is caused by double reflection from the feed and the antenna.

Measured radiation patterns are shown in Fig. 11. The measured patterns agree well with the designed ones. The measured beamwidth is listed in Table 4. The difference of the beamwidth between E- and H-planes is less than 2.5°. The WG-MSL transition is covered by an absorber during the measurement to exclude radiation from the transition.

A back-to-back WG-MSL transition was fabricated as shown in Fig. 12 to estimate insertion loss of the feed circuit and the gain of the antenna itself. Measured frequency characteristics of the insertion loss are shown in Fig. 13. The insertion loss is 1.8 to 2.1 dB in the target bandwidth. tan δ of the substrate is estimated by simulation with different value of tan δ while its conductivity is kept 2.0×10^7 S/m. The estimated tan δ of the substrate is 0.0081. The insertion

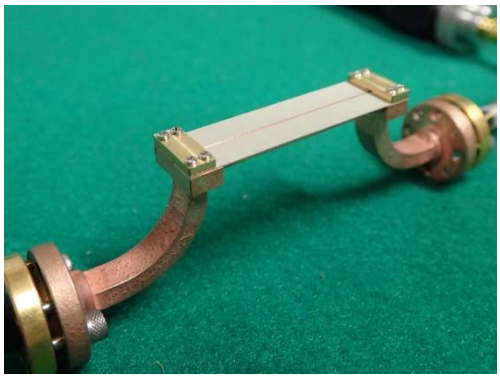

Fig. 12 Fabricated back-to-back WG-MSL transition.

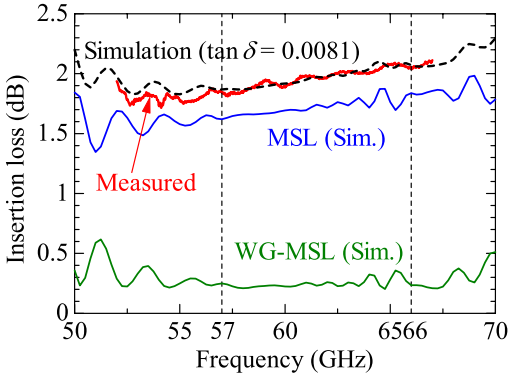

Fig. 13 Frequency characteristics of insertion loss.

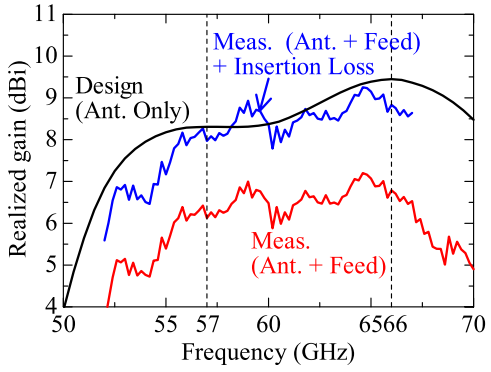

Fig. 14 Frequency characteristic of gain.

loss of WG-MSL transition and MSL is simulated as shown in Fig. 13 and is 0.2 dB and 1.7 dB at 61.5 GHz, respectively. The unit loss of MSL is 0.09 dB/mm. When the antenna is integrated with an integrated chip, the insertion loss can be suppressed by shortening the distance between the antenna and the chip. Another solution to reduce the insertion loss is to use low tan δ substrate such as PTFE or alumina because the unit loss decreases up to 0.03 dB/mm with tan δ of 0.001.

Measured frequency characteristics of gain are shown in Fig. 14. The gain of antenna itself is estimated as sum of the measured gain and the measured insertion loss of the feed circuit as plotted in the same figure. Similar tendency

Table 5 Dimension and performance comparison of the proposed metal cap slot antenna with other 60-GHz band endfire antennas on a substrate†.

Ref.	Type	Length (mm)	Width (mm)	Thickness (mm)	Gain (dBi)	Reflection (<−10dB) BW (%)
[8]	Patch array	0.6	18.4	NA	10.9	7.8
This work	Slot array	2.5	8.0	4.5	9.3	29.1
[5]	Dipole array	3.0	12.0	0.3	9.5	26.7
[7]*	Dipole array	3.2	6.5	2.3	9.8	25.8
[6]	Dipole array	3.5	11.32	4.7	13.1	22.1
[12]	Substrate slab	5.0	8.4	1.0	10.0	14.6
[10]	Taper slot array	5.3	2.4	0.1	9.9	25.2
[4]	Yagi-Uda	7.0	8.0	0.3	10.8	17.0
[9]	Bow-tie	7.5	8.5	0.5	12.0	8.1
[11]	Horn	24.0	20.0	1.4	14.6	10.5

of the antenna gain was observed between the designed and estimated ones. The antenna gain is larger than 7.8 dBi in the target bandwidth.

Comparison of 60-GHz band endfire antennas on a substrate is shown in Table 5. The proposed antenna realized the second shortest length in radiation direction and the widest reflection bandwidth with comparable gain. The patch antenna array [7] has the shortest length but it suffers narrow bandwidth to cover entire 60-GHz band. The thickness of the proposed antenna is the second thickest among the antennas. Because radiation elements of the other antennas are exposed, reflection and radiation characteristics are disturbed when an object is placed around the antenna. In [4], it was shown that 5-mm (one free space wavelength) displacement from radiation elements is required not to disturb antenna characteristics. Therefore, the effective thickness of the other antennas are 10 mm or 5 mm (one side of the substrate is metaled). We can conclude that the thickness of the proposed antenna is comparable or less with the other antennas.

5. Conclusion

In this paper, we have proposed a metal cap antenna for the 60-GHz band. The dimension of the designed antenna is $8.0 \times 4.5 \times 2.5$ mm^3 and was fabricated by machining a brass block. The antenna has shown robustness on the fabrication tolerance and effects from surrounding objects. The measured reflection is less than −10.0 dB and the realized gain is larger than 7.8 dBi over the target bandwidth. The half power beamwidth on both E- and H-plane is between 54°–65° with endfire radiation over the target bandwidth. The antenna showed high gain together with short length in the

†The dimension does not include feed circuit parts. The length is the radiating direction dimension. The width is the dimension perpendicular to both radiation direction and the substrate. The length is the dimension perpendicular to radiation direction and parallel to the substrate.

*The dimensions are scaled down from 28.0 GHz to 61.5 GHz for the comparison.

radiation direction. This antenna also can be integrated with PCB because it is insensitive with metal blocks behind it. The antenna is suitable for mobile terminals such as smart phones and tablets.

References

[1] R. Fisher, "60 GHz WPAN standardization within IEEE 802.15.3c," Proc. Int. Signals, Syst. Electron. Symp., pp.103–105, 2007. DOI: 10.1109/ISSSE.2007.4294424
[2] R. Willmot, D. Kim, and D. Peroulis, "A Yagi–Uda array of high efficiency wire-bond antennas for on-chip radio applications," IEEE Trans. Microw. Theory Techn., vol.57, no.12, pp.3315–3321, Dec. 2009. DOI: 10.1109/TMTT.2009.2034051
[3] S.-S. Hsu, K.-C. Wei, C.-Y. Hsu, and H.-R. Chuang, "A 60-GHz millimeter-wave CPW-fed Yagi antenna fabricated by using 0.18 μm CMOS technology," IEEE Electron Device Lett., vol.29, no.6, pp.625–627, June 2008. DOI: 10.1109/LED.2008.920852
[4] R.A. Alhalabi, Y.C. Chiou, and G.M. Rebeiz, "Self-shielded high-efficiency Yagi-Uda antennas for 60 GHz communications," IEEE Trans. Antennas Propag., vol.59, no.3, pp.742–750, March 2011. DOI: 10.1109/TAP.2010.2103032
[5] A. Lamminen and J. Säily, "Wideband millimetre wave end-fire antenna and array for wireless short-range applications," Proc. 5th Eur. Conf. Antennas Propag., pp.1–5, 2010.
[6] J. Wang, Y. Li, L. Ge, J. Wang, and K.M. Luk, "A 60 GHz horizontally polarized magnetoelectric dipole antenna array with 2-D multibeam endfire radiation," IEEE Trans. Antennas Propag., vol.65, no.11, pp.5837–5845, Nov. 2017. DOI: 10.1109/TAP.2017.2754328
[7] W. El-Halwagy, R. Mirzavand, J. Melzer, M. Hossain, and P. Mousavi, "Investigation of wideband substrate-integrated vertically-polarized electric dipole antenna and arrays for mm-wave 5G mobile devices," IEEE Access, vol.6, pp.2145–2157, 2018. DOI: 10.1109/ACCESS.2017.2782083
[8] W. Hong, K.H. Baek, and S. Ko, "Millimeter-wave 5G antennas for smartphones: Overview and experimental demonstration," IEEE Trans. Antennas Propag., vol.65, no.12, pp.6250–6261, Dec. 2017. DOI: 10.1109/TAP.2017.2740963
[9] A. Dadgarpour, B. Zarghooni, B.S. Virdee, and T.A. Denidni, "Millimeter-wave high-gain SIW end-fire bow-tie antenna," IEEE Trans. Antennas Propag., vol.63, no.5, pp.2337–2342, May 2015. DOI: 10.1109/TAP.2015.2406916
[10] L. Pazin and Y. Leviatan, "A compact 60-GHz tapered slot antenna printed on LCP substrate for WPAN applications," IEEE Antennas Wireless Propag. Lett., vol.9, pp.272–275, 2010. DOI: 10.1109/LAWP.2010.2046612
[11] B. Pan, Y. Li, G.E. Ponchak, J. Papapolymerou and M.M. Tentzeris, "A 60-GHz CPW-fed high-gain and broadband integrated horn antenna," IEEE Trans. Antennas Propag., vol.57, no.4, pp.1050–1056, April 2009. DOI: 10.1109/TAP.2009.2015815
[12] R. Suga, H. Nakano, Y. Hirachi, J. Hirokawa, and M. Ando, "A small package with 46-dB isolation between Tx and Rx antennas suitable for 60-GHz WPAN module," IEEE Trans. Microw. Theory Techn., vol.60, no.3, pp.640–646, March 2012. DOI: 10.1109/TMTT.2011.2181535
[13] K. Ito, J. Hirokawa, K. Sakurai, and M. Ando, "Metal cap with two slots covering an edge of a mobile device substrate for 60 GHz band," Proc. Intl. Synp. Antenna Propagat., TH1D-03, Dec. 2014. DOI: 10.1109/ISANP.2014.7026611
[14] H. Hirayama, J. Hirokawa, and M. Ando, "Design for the feeding structure of a metal cap with two slots attaching at the edge of a mobile module substrate for 60 GHz band," Proc. Intl. Synp. Antenna Propagat., POS1-31, pp.346–347, Oct. 2016.
[15] N. Marcuvitz, Waveguide Handbook, Peter Peregrinus, London, 1986.
[16] Y. Deguchi, K. Sakakibara, N. Kikuma, and H. Hirayama, "Design and optimization of millimeter-wave microstrip-to-waveguide transition operating over broad frequency bandwidth," IEICE Trans. Electron., vol.E90-C, no.1, pp.157–164, Jan. 2007.

Takashi Tomura received the B.S., M.S. and D.E. degrees in electrical and electronic engineering from the Tokyo Institute of Technology, Tokyo, Japan, in 2008, 2011 and 2014, respectively. He was a Research Fellow of the Japan Society for the Promotion of Science (JSPS) in 2013. From 2014 to 2017, he worked at Mitsubishi Electric Corporation, Tokyo and was engaged in research and development of aperture antennas for satellite communications and radar systems. He is currently a Specially Appointed Assistant Professor at the Tokyo Institute of Technology, Tokyo. His research interests include electromagnetic analysis, aperture antennas and planar waveguide slot array antennas. Dr. Tomura received the Best Student Award from Ericsson Japan in 2012 and the IEEE AP-S Tokyo Chapter Young Engineer Award in 2015. He is a member of the IEICE.

Haruhisa Hirayama received B.E. degrees in Information and Communication Engineering from Tokyo Metropolitan University in 2015 and M.E. degrees in Electrical and Electronic Engineering from Tokyo Institute of Technology in 2017. He joined KDDI CORPORATION in 2017, where he was engaged in LTE network operation.

Jiro Hirokawa received the B.S., M.S. and D.E. degrees in electrical and electronic engineering from Tokyo Institute of Technology (Tokyo Tech), Tokyo, Japan in 1988, 1990 and 1994, respectively. He was a Research Associate from 1990 to 1996 and an Associate Professor from 1996 to 2015 at Tokyo Tech. He is currently a Professor there. He was with the antenna group of Chalmers University of Technology, Gothenburg, Sweden, as a Postdoctoral Fellow from 1994 to 1995. His research area has been in slotted waveguide array antennas and millimeter-wave antennas. He received IEEE AP-S Tokyo Chapter Young Engineer Award in 1991, Young Engineer Award from IEICE in 1996, Tokyo Tech Award for Challenging Research in 2003, Young Scientists' Prize from the Minister of Education, Cultures, Sports, Science and Technology in Japan in 2005, Best Paper Award in 2007 and a Best Letter Award in 2009 from IEICE Communications Society, and IEICE Best Paper Award in 2016 and 2018. He is a Fellow of IEEE.